Supporting Information

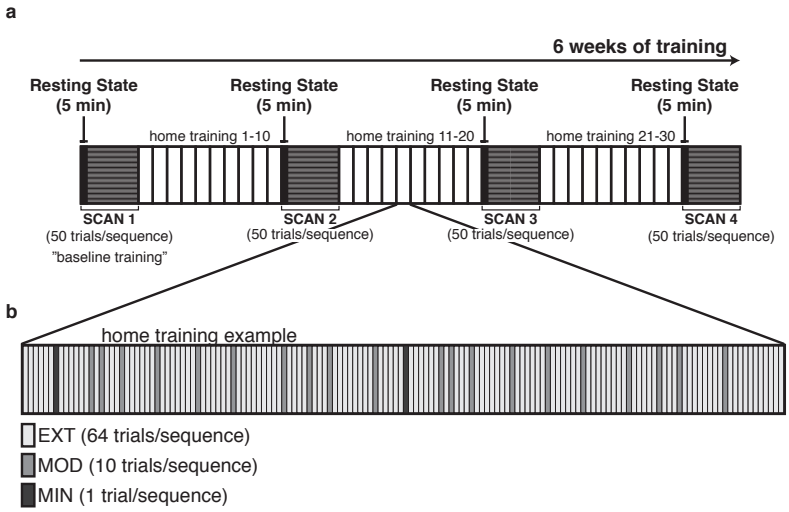

Figure S1: **Experiment protocol and timeline.**
(a) The experiment protocol comprised of six weeks of training of six distinct motor sequences. Following a brief explanation of the task instructions, an initial MRI scan session was held during which blood-oxygen-level dependent (BOLD) signals were acquired from each participant. The scan session began with a resting state scan lasting 5 minutes where participants were instructed to remain awake and with eyes open without fixation. During the remainder of the first scan session (baseline training), participants practiced each of six distinct motor sequences for 50 trials each, or approximately 1.5 hours. They were then instructed to continue practicing the motor sequences at home using a training module that was installed by the experimenter (N.F.W.) on their personal laptops. Participants completed a minimum of 30 home training sessions, which were interleaved with two additional scan sessions, each occurring after at least 10 home training sessions. A final scan session was held following the completion of the 6 weeks of training. The same protocol was followed in each of the four scan sessions: a 5 minute resting state scan, followed by approximately 1.5 hours of the DSP task, where each of six distinct motor sequences was practiced for 50 trials each.
(b) Most of the motor sequence training occurred at home, between scanning sessions. An ideal home training session consisted of 150 trials with sequences practiced in random order (randomization used the Mersenne Twister algorithm of Nishimura and Matsumoto as implemented in the random-number generator rand.m of MATLAB version 7.1). Each EXT sequence was practiced for 64 trials, each MOD sequence was practiced for 10 trials, and each MIN sequence was practiced for 1 trial.

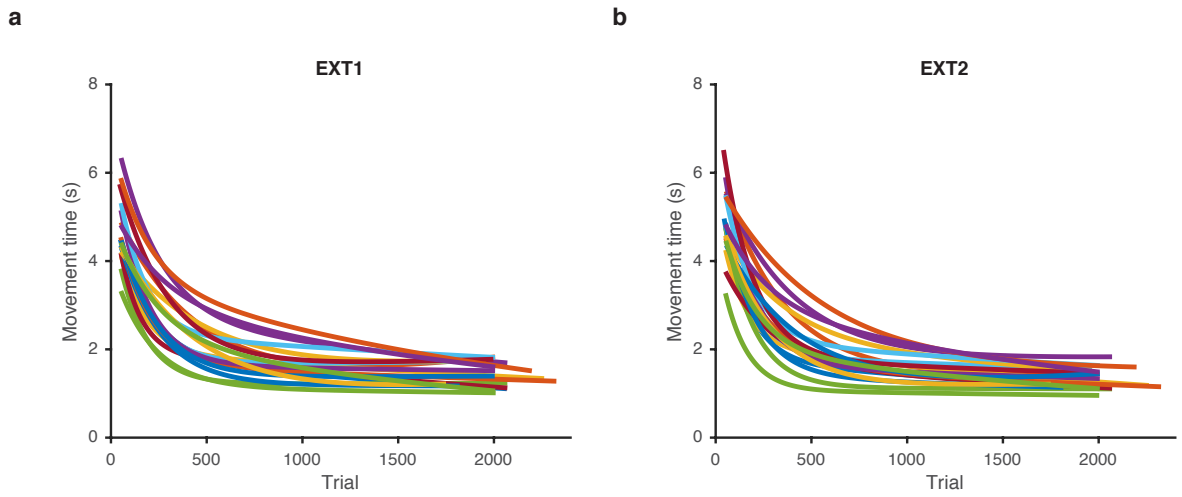

Figure S2: **Learning curves from individual participants.** Time required to execute a complete motor sequence (*movement time*), as a function of trial number. Colored curves are two-term exponential fits of the movement times from each participant. Learning happened for all participants, as evidenced by the reduction of movement times, but with large variability in the decay rates.
(a) EXT1 sequence.
(b) EXT2 sequence.

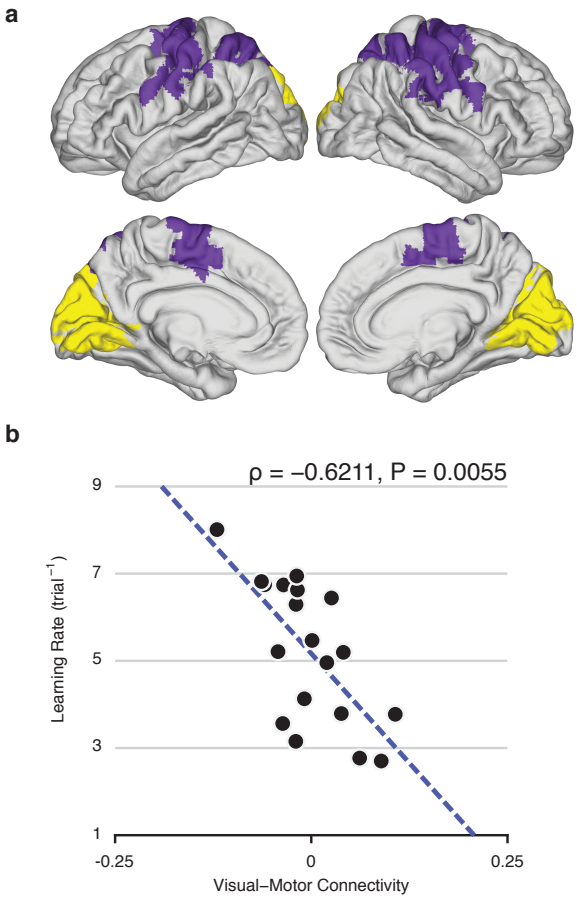

Figure S3: **Replication of Figure 2 using an anatomical parcellation (AAL-626).** *(a)* Visual module (yellow) and somato-motor module (purple), identified by time-resolved clustering methods applied to BOLD activity acquired during the execution of motor sequences (Bassett et al., 2015). The modules were defined in a data-driven manner and correspond broadly but not exactly to putative visual and somato-motor modules. *(b)* Functional connectivity between visual and somato-motor modules, estimated at rest and prior to learning, reliably predicts individual differences in future learning rate. We define the learning rate as the exponential drop-off parameter of the participant's movement time as a function of trials practiced, and we define functional connectivity as the average correlation value between activity in visual regions and somato-motor regions.

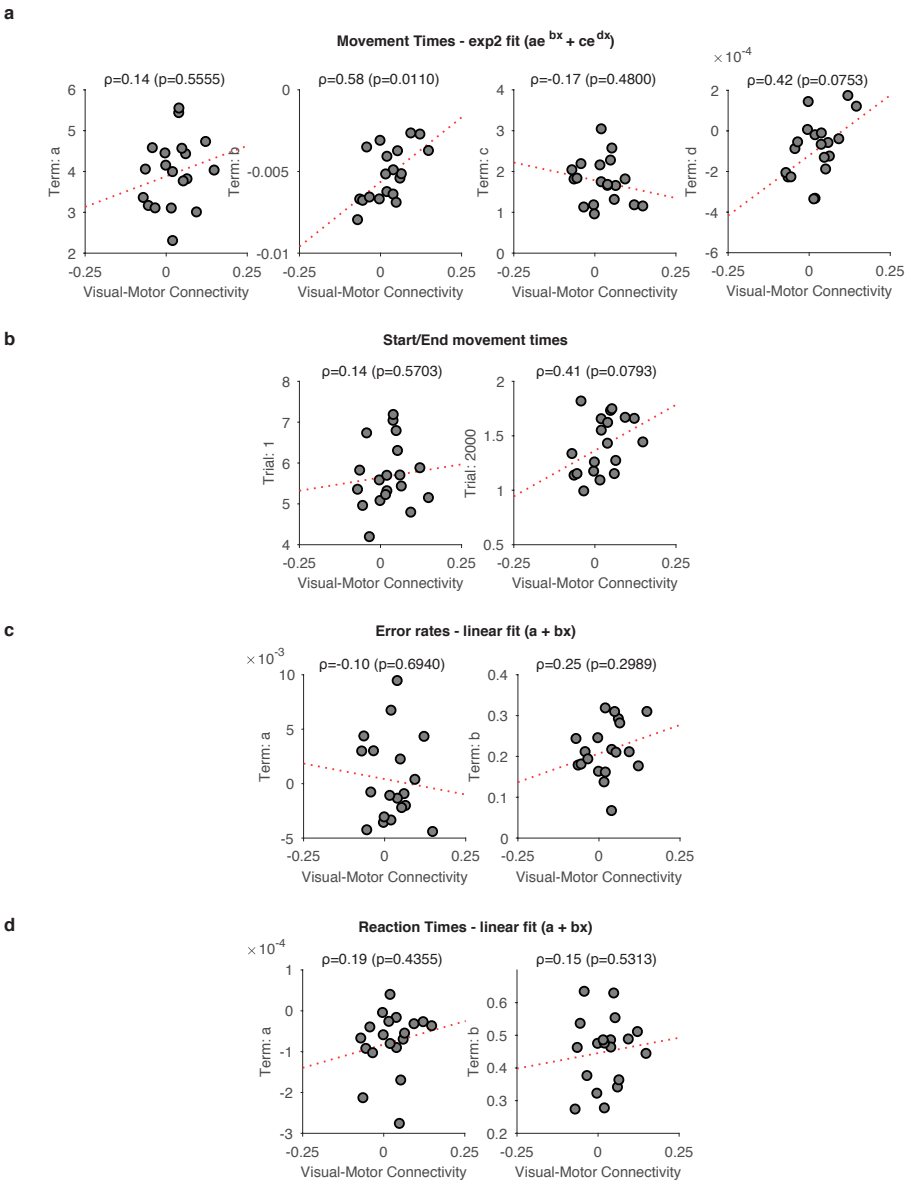

Figure S4: **Statistical relationship between resting visual-motor connectivity and different behavioral markers.**
(a) Relationship between resting-state visual-motor connectivity estimated from the resting-state scan acquired in SESSION 1 and each of the four parameters from the two-term exponential fits of the movement times. Notice the marginal significance of the correlation between visual-motor connectivity and *term d*, suggesting that visual-motor connectivity correlates not only with the faster drop-off parameter (*term b*), but also with the slower decay parameter (*term d*).
(b) Relationship between resting-state visual-motor connectivity estimated from the resting-state scan acquired in SESSION 1 and the fitted start movement time (*left*); similarly for fitted end movement time (*right*). Notice the marginal significance of the correlation between visual-motor connectivity and movement time at trial 2000, suggesting that participants with high visual-motor connectivity tend to have longer movement times at the end of the training session.
(c) Relationship between resting-state visual-motor connectivity estimated from the resting-state scan acquired in SESSION 1 and both parameters from a linear fit to the error rates.
(d) Relationship between resting-state visual-motor connectivity estimated from the resting-state scan acquired in SESSION 1 and both parameters from a linear fit to the reaction times.

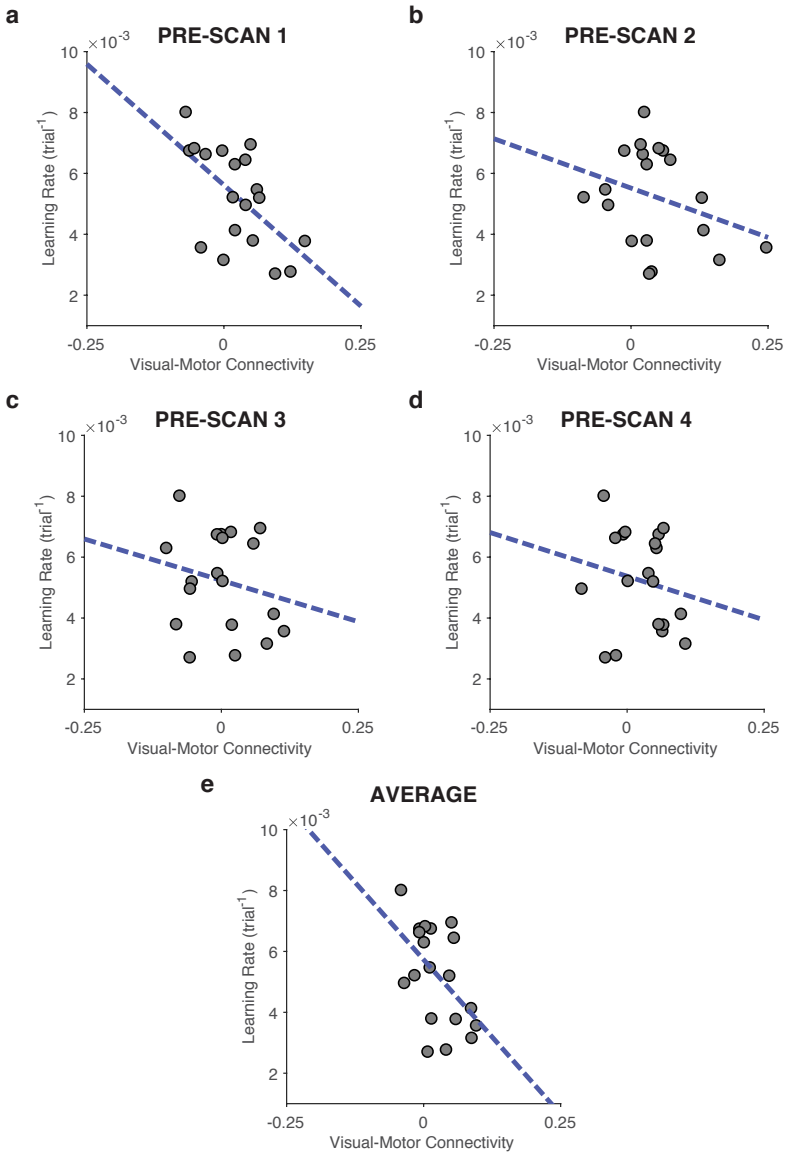

Figure S5: **Correlation between visual-motor connectivity at various sessions and overall learning rate.**
(a) Relationship between visual-motor connectivity estimated from the resting-state scan acquired in SESSION 1 and overall learning rate. The Spearman correlation between these two quantities is $\rho = -0.5772, P = 0.0110$.
(b) Relationship between visual-motor connectivity estimated from the resting-state scan acquired in SESSION 2 and overall learning rate. The Spearman correlation between these two quantities is $\rho = -0.2895, P = 0.2286$.
(c) Relationship between visual-motor connectivity estimated from the resting-state scan acquired in SESSION 3 and overall learning rate. The Spearman correlation between these two quantities is $\rho = -0.1772, P = 0.4664$.
(d) Relationship between visual-motor connectivity estimated from the resting-state scan acquired in SESSION 4 and overall learning rate. The Spearman correlation between these two quantities is $\rho = -0.1561, P = 0.5218$.
(e) Relationship between average visual-motor connectivity across all four sessions and overall learning rate. The Spearman correlation between these two quantities is $\rho = -0.4614, P = 0.0484$.

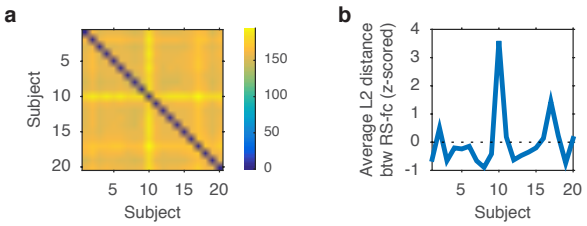

Figure S6: **Subject exclusion criterion.**
(a) We examined resting-state data quality by tracking functional connectivity outliers from our group norm. We calculated the average L2 distance between corresponding cells of the 626×626 functional connectivity matrices from all pairs of participants, summarized in the dissimilarity matrix of the figure.
(b) Average L2 distance between the RSFC matrix of one participant and that from all others. With the exception of subject 10, all subjects were within 1.5 standard deviations from each other. The resting state data from subject 10 differed on average by 3.6 standard deviations from the others and, therefore, was excluded from the remainder of the analyses.

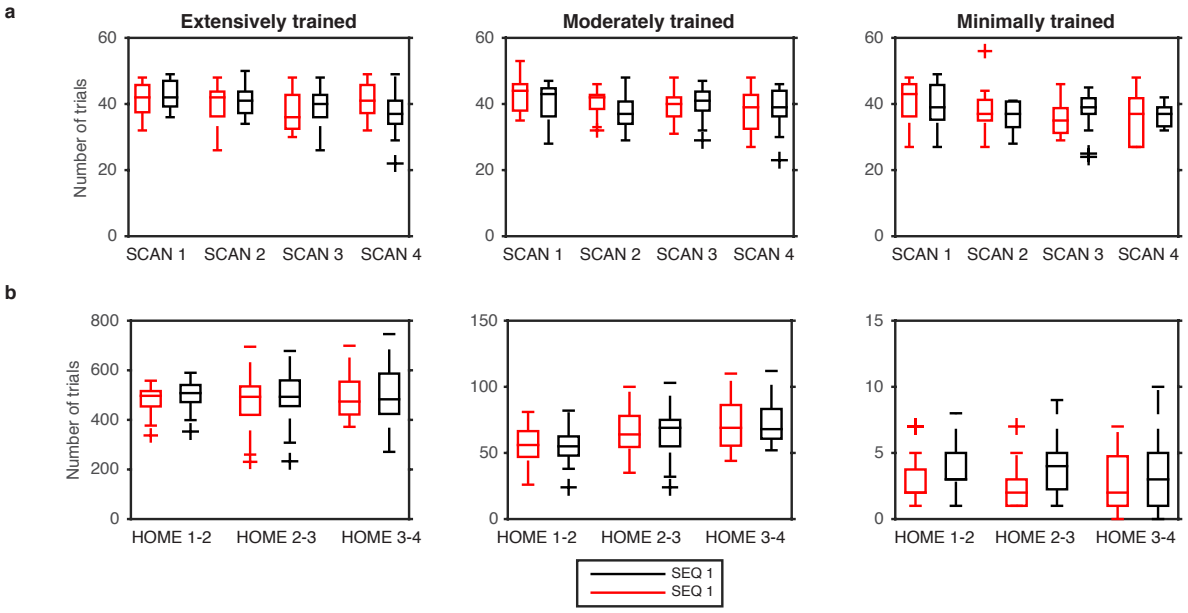

Figure S7: **Number of error-free trials performed per session.**
(a) Number of trials practiced in each scan session. *Left panel:* Extensive training (EXT) session; *Middle panel:* Moderate training (MOD) session; *Right panel:* Minimal training (MIN) session. Box plot represents quartiles and the '+' symbols represent outliers. The variability in the number of executed trials during scan sessions arose mainly due to software or hardware difficulties.
(b) Number of trials practiced in each home session. *Left panel:* Extensive training (EXT) session; *Middle panel:* Moderate training (MOD) session; *Right panel:* Minimal training (MIN) session. Box plot represents quartiles and the '+' symbols represent outliers. The variability in the number of executed trials is due to some subjects training more days than others between successive scanning sessions.

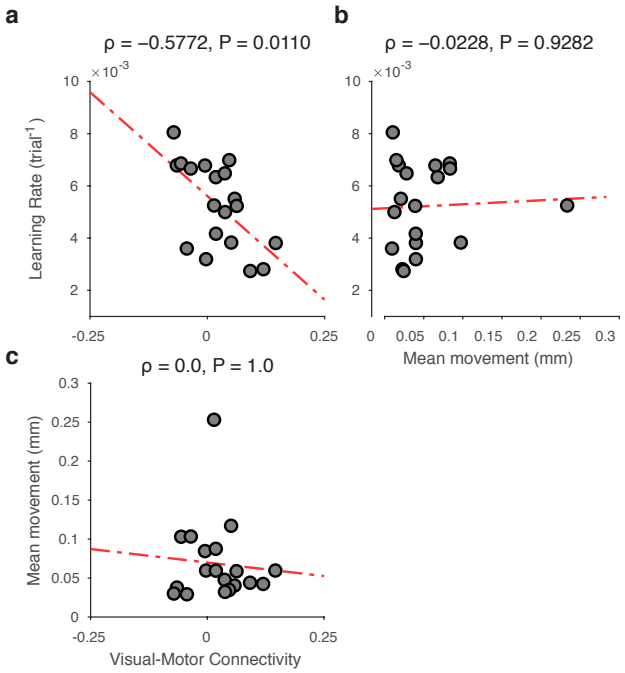

Figure S8: **Pairwise relationships between mean subject motion, visual-motor connectivity, and learning rate.**
(a) Relationship between visual-motor connectivity (in session 1) and learning rate — as in Fig. 2.
(b) Relationship between mean subject motion (in session 1) and learning rate. Learning rate was unrelated to subject motion.
(c) Relationship between visual-motor connectivity (in session 1) and mean subject motion. Visual-motor connectivity was unrelated to subject motion.

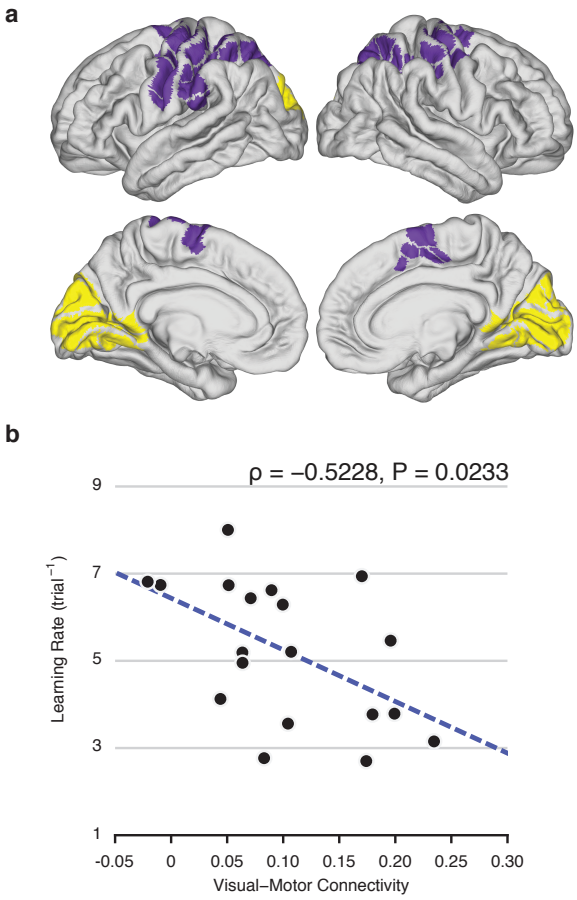

Figure S9: **Replication of Fig. 2 with uncentered functional connectivity values.**
(a) Same as Fig. 2a: Visual (yellow) and somato-motor (purple) modules.
(b) Similar to Fig. 2b. The removal of various signal components present throughout most of the brain (in particular by the *tCompCor* method) leads to a shift of the distribution of functional connectivity values, giving rise to negative correlations (Fig. 2b). Here, we use a less stringent noise removal pipeline (same as the original but without the *tCompCor* method) that produces a smaller shift of the range of correlation values. In line with our original results, we observe that functional connectivity between visual and somato-motor modules, estimated at rest and prior to learning, reliably predicts individual differences in future learning rate ($\rho = -0.5280$, $P = 0.02174$). The slightly weaker statistical relationship is likely a consequence of residual physiological noise (Lund and Hanson, 2001).

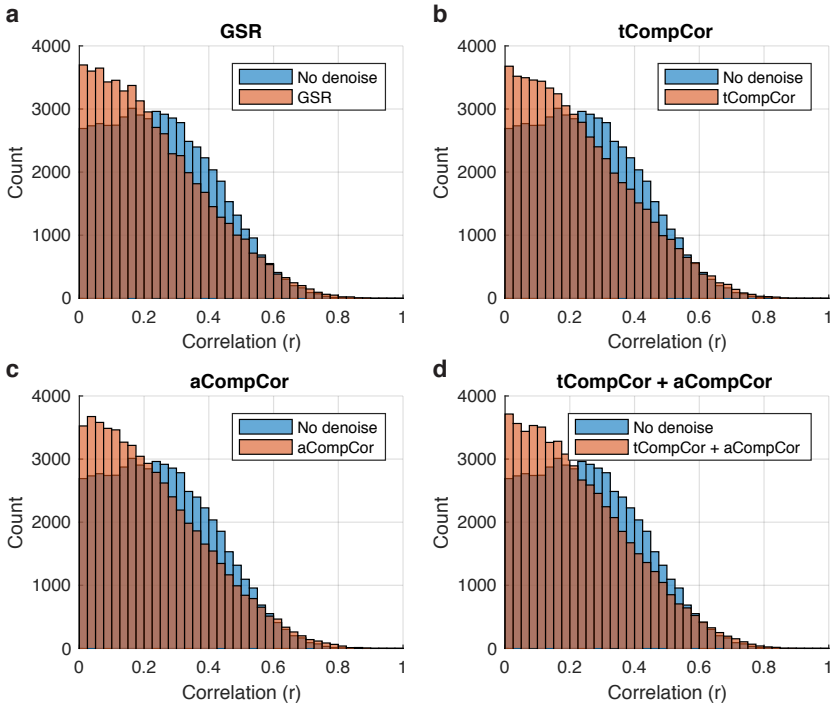

Figure S10: **Distribution of correlation values between individual differences in subject mean motion and edge weight for different preprocessing procedures.**
(a) Global-signal regression (GSR).
(b) tCompCor (Behzadi et al., 2007).
(c) aCompCor (Behzadi et al., 2007).
(d) A combination of tCompCor and aCompCor (Behzadi et al., 2007).